IEEE Access
Multidisciplinary | Rapid Review | Open Access Journal

Date of publication xxxx 00, 0000, date of current version xxxx 00, 0000.

Digital Object Identifier 10.1109/ACCESS.2022.Doi Number

Mechanism of Conversion Between AC and DC Electrical Variables in LCC Main Circuits During Grid Dynamics Using Time-Varying Amplitude/Frequency Rotating Vectors

SHUCHAN HE[1], XIAOMING YUAN[1], (Senior Member, IEEE), JIABING HU[1], (Senior Member, IEEE), and HUI YANG[1]

[1]School of Electrical and Electronic Engineering, Huazhong University of Science and Technology, Wuhan 430074, China

Corresponding author: SHUCHAN HE (e-mail: csps_hsc@ hust.edu.cn).

This work was supported by the Science and Technology Project of State Grid, HUST-State Grid Future of Grid Institute under Grant 5100-202199548A-0-5-ZN.

ABSTRACT With the increasing challenges posed by line-commutated converter-based high-voltage direct current (LCC-HVDC) in the era of widespread renewable energy utilization, AC/DC dynamic interaction problems under controller regulations appeared more often. However traditional approaches often fall short in identifying the features of signals involved in AC/DC conversion in grid dynamics, and the characteristics of the conversion process in the LCC main circuit are overlooked. Consequently, this paper aims to fill this gap to help reveal the mechanism of grid dynamic problems dominated by controller regulations. Based on the recognition that the amplitude/frequency of AC electrical variables has time-varying characteristics in practice during grid dynamics, this paper focuses on the conversion mechanism between AC and DC electrical variables and then the basic features of electrical variables in LCC main circuits during grid dynamics are expressed using time-varying amplitude/frequency rotating vectors. First, the six-pulse firing pattern is expressed using the rotating vector with time-varying frequency. Then the time-varying amplitude/frequency rotating vectors are utilized to discuss how AC/DC voltage and current converse, including the power produced from them during grid dynamics. Moreover, simulations are performed to validate the efficacy of the mechanism, alongside elucidating its potential applications to benefit grid dynamic analysis. Finally, the salient contributions of this proposed framework are clarified.

INDEX TERMS Amplitude/frequency, conversion mechanism, circuits, grid dynamics, LCC, rotating vectors, time-varying.

I. INTRODUCTION

With the step increasingly deployed line-commutated converter-based high-voltage direct current (LCC-HVDC) for long distance electricity transmission to eastern China, the sending-end grid in western China is also under continued large scale development of renewable generations. It is expected to face unprecedented challenges especially voltage and frequency stability problems, as well as wide frequency range oscillations [1]-[2].

Aforementioned grid dynamic challenges are within the context of the interaction between AC and DC grids, naming as AC/DC interaction problems [3]-[5]. With the large-scale penetration of renewable energy, the grid AC/DC interaction problems regulated by LCC direct current/direct voltage/extinction angle control, have faster dynamics than they have in traditional power system. However, existing works rooted in traditional power systems fail to adequately capture the evolving intricacies of AC/DC interaction dynamics, leading to their insufficiency to adapt to the present grid operations [1]. There arises a pressing need to understand how to depict AC/DC interactions dynamics which poses significant threats to the operational safety and stability of the current power system [6]-[10]. Given that AC/DC interactions are inherent to the thyristor circuit-based AC/DC conversion within LCC converter stations, it becomes necessary to

explain clearly the manner in which AC and DC electrical variables converse, particularly during grid dynamics.

There have been several works about how AC and DC electrical variables converse in LCC main circuits, typically categorized into two aspects: 1) phasor-based description; 2) harmonic description.

The phasor-based description assumes that AC voltage's amplitude and phase vary slowly and the frequency remains constant during AC/DC conversion [11]. In this framework, phasors derived from sinusoidal steady-state analysis are employed to geometrically depict AC voltage. However, this approach is rational for standard sinusoidal waveform, confined to the sinusoidal steady-state condition instead of practical grid dynamic process [12], [22].

The harmonic description relies on the superposition of harmonics derived from Fourier series to characterize AC signals [13]. However, the theory of Fourier series is specifically designed for periodic signals [14], [23]. That is to say, during AC/DC conversion, harmonic description's application is limited to the periodic condition. In practical grid dynamics, AC instantaneous value signals are the non-periodic signals which exhibit a continuous spectrums with no match to the harmonic disturbance [15]-[16].

Consequently, the aforementioned two descriptions are strictly applicable to the depiction of steady-state system. In traditional power systems dominated by synchronous machines, the time scale of dynamics is quite slow. Hence, the phasor-based description and harmonic description may have their application scenarios rationality when applying for grid dynamics analysis. However, in modern power system along with the high penetration of the power electronics devices, the time scale of dynamics becomes faster owing to the fast controls effect [17]. It seems somewhat irrational to deal with the dynamic problems directly based on the traditional methods. In addition, accurately describing how the AC and DC electrical variables converse can utilize the AC/DC instantaneous values based on the switching functions [18]. But relying solely on mathematical switching functions containing the discrete switching dynamics may not suffice to fully elucidate the in-depth operational mechanisms [19]. Hence, it becomes imperative to contemplate how to portray the AC/DC conversion process during grid dynamics now.

Why do existing researches lack comprehensive understandings of AC/DC conversion adapted to the present grid dynamics? The primary reason may lies in the insufficient understanding of the signal characteristics of AC electrical variables, such as AC voltages and AC currents, in the grid dynamic processes. During grid dynamic operation, different types of devices exchange active/reactive power with the network, and then the amplitude/frequency of internal voltages are characterized by time-varying values under the effect of devices regulation [15], [17]. AC currents flowing through the network exhibit time-varying amplitude/frequency characteristics under the excitation of time-varying amplitude/frequency internal voltages [17]. Consequently, AC signals possess the nature of time-varying amplitude and frequency during dynamics.

In practical LCC main circuits, the station's AC voltage affects the DC voltage and then DC current dominates AC current's amplitude [18]. Meanwhile, the firing angle order and the phase-locked loop (PLL) position work to generate AC current's phase and frequency [18]. So the station naturally outputs AC current with time-varying amplitude and frequency. Meanwhile, grid-tied devices regulate AC voltage amplitude and frequency to realize the function of power transmission, so that the voltage's stable amplitude and frequency serve as the objectives of the power system operation, which provide a platform to physically evaluate the station's influence on the grid dynamics [17]. As a result, focusing on AC signals' time-varying amplitude and frequency helps reveal the features governing how and why AC/DC conversion is that in LCC main circuits, which benefits to grid dynamic analysis.

In this paper, based on the recognition that the amplitude/frequency (A/F) of AC electrical variables has time-varying characteristics in practice during grid dynamic process, the six-pulse firing pattern as well as the AC voltage and current are expressed using the time-varying A/F rotating vectors. Then rotating vectors are utilized to discuss the correlations between AC/DC voltage and current. The applications of the proposed mechanism are also presented, including the revised "rotating phasor", the physical generation of active/reactive power in grid dynamics, and the link with future research on station characteristics. Finally, simulations are performed to validate the efficacy and the salient contributions of this proposed framework are clarified.

II. AMPLITUDE/FREQUENCY TIME-VARYING NATURE OF THE AC SIGNALS DYNAMICS DESCRIBED USING TIME-VARYING AMPLITUDE/FREQUENCY ROTATING VECTORS

This section aims to explain the A/F time-varying nature of the AC signals whose dynamics are described using time-varying A/F rotating vectors, so as to prepare for researching conversion mechanism between electrical variables. First, the AC-DC voltage and current relationships in LCC main circuits based on switching functions are introduced [20]. Then the AC voltage, the firing pulse pattern, and the AC current from these relationships are clarified with time-varying A/F. Finally, the dynamics of the AC voltage, the firing pulse pattern, and the AC current can be described using the corresponding time-varying A/F rotating vectors.

A. AC-DC VOLTAGE/CURRENT SWITCHING FUNCTIONS RELATIONSHIPS

Switching function theory claims the AC-DC voltage and current relationship of a 6-pulse converter bridge ignoring the commutation process [20], which are derived as

$$v_{\mathrm{d}} = v_{\mathrm{ab}} S_{\mathrm{ab}} + v_{\mathrm{bc}} S_{\mathrm{bc}} + v_{\mathrm{ca}} S_{\mathrm{ca}} \quad (11)$$

$$i_{\mathrm{k}} = i_{\mathrm{d}} S_{\mathrm{k}} (\mathrm{k} = \mathrm{a}, \mathrm{b}, \mathrm{c}) \quad (22)$$

where v_{ab}, v_{bc}, v_{ca} and i_{k} are the line voltage and phase current of the AC side of the converter. v_{d}, i_{d} are the direct voltage and current of the converter. (S_{ab}, S_{bc}, S_{ca}) and S_{k} represent the switching functions for voltage and current, respectively. The switching functions $S_{\mathrm{ab/bc/ca}}$ (combination of S_{ab}, S_{bc}, S_{ca}) and $S_{\mathrm{a/b/c}}$ (combination of S_{a}, S_{b}, S_{c}) are shown in Fig. 1, where α refers to the actual firing angle. It's important to note that $S_{\mathrm{ab/bc/ca}}$ (or $S_{\mathrm{a/b/c}}$) differs in phase by $2\pi/3$ with each other.

B. AMPLITUDE/FREQUENCY TIME-VARYING NATURE OF AC VOLTAGE

The instantaneous value of the AC voltage is the projection of the A/F-generated voltage rotating vector passing through an oscillator on the coordinate axis, with the A/F determining the vector length and angular velocity, respectively [17]. The projections of the line voltage rotating vector on the ab, bc, and ca axes, which differ from each other by $2\pi/3$, form $v_{\mathrm{ab/bc/ca}}$. Therefore, v_{ab}, v_{bc}, and v_{ca} have the same A/F but differ in phase by $2\pi/3$ at any time, as shown in Fig. 2. The expression of v_{ab}, v_{bc}, and v_{ca} are as follows.

$$\begin{cases} v_{\mathrm{ab}} = A(t)\cos\left(\int_{t_0}^{t} \omega\ (t)\mathrm{d}t + \theta_{\mathrm{e0}}\right) \\ v_{\mathrm{bc}} = A(t)\cos\left(\int_{t_0}^{t} \omega\ (t)\mathrm{d}t + \theta_{\mathrm{e0}} - \frac{2}{3}\pi\right) \\ v_{\mathrm{ca}} = A(t)\cos\left(\int_{t_0}^{t} \omega\ (t)\mathrm{d}t + \theta_{\mathrm{e0}} + \frac{2}{3}\pi\right) \end{cases} \quad (33)$$

So that (3) work together to form AC voltage rotating vector $\boldsymbol{v}_{\mathrm{line}}$, as (4) shows.

$$\boldsymbol{v}_{\mathrm{line}} = v_{\mathrm{ab}} + v_{\mathrm{bc}} e^{j(2\pi/3)} + v_{\mathrm{ca}} e^{j(4\pi/3)} \quad (44)$$

C. FREQUENCY TIME-VARYING NATURE OF FIRING PULSE PATTERN

When the phase of PLL's sawtooth wave is equal to the firing angle order, a firing pulse is triggered [18]. The time-varying frequency of the AC voltage indicates that the PLL's frequency is also time-varying. Therefore, the phase of the sawtooth wave and the firing angle order are expressed as

$$\begin{cases} \theta_{\mathrm{pll}}(t_{\mathrm{k}}) = \omega_0 t_{\mathrm{k}} - k\pi/3 + \theta_{\mathrm{pll0}} + \Delta\theta_{\mathrm{pll}}(t_{\mathrm{k}}) \\ \alpha_0(t_{\mathrm{k}}) = \alpha_{0\_\mathrm{steady}} + \Delta\alpha_0(t_{\mathrm{k}}) \end{cases} \quad (55)$$

where θ_{pll0} is the initial PLL phase. $\Delta\theta_{\mathrm{pll}}$ is the PLL's phase disturbance. $\alpha_{0\_\mathrm{steady}}$ is the firing angle order in the steady state, and $\Delta\alpha_0$ is the disturbance of the firing angle order.

Suppose that t_1 and t_2 are the triggering moments of two adjacent firing pulses. Then, (5) implies that

$$\theta_{\mathrm{pll}}(t_1) = \alpha_0(t_1), \theta_{\mathrm{pll}}(t_2) = \alpha_0(t_2)$$
$$\Rightarrow \left(\omega_0 t + \Delta\theta_{\mathrm{pll}} - \Delta\alpha_0\right)\Big|_{t_1}^{t_2} = \frac{\pi}{3} \Rightarrow \int_{t_1}^{t_2} \omega_{\mathrm{d}} dt = \frac{\pi}{3} \quad (66)$$

In (6), dynamics of the firing pulse can be described using the pulsed rotating vector. The frequency of the vector is

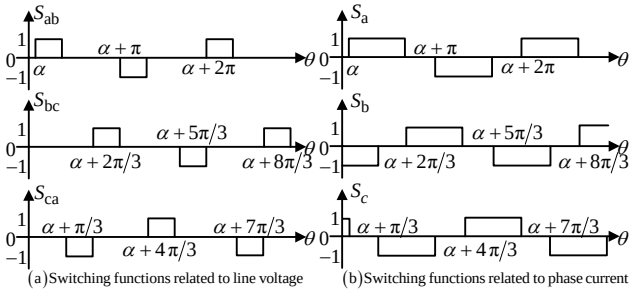

FIGURE 1. Waveforms of switching functions related to line voltage S_{ab}, S_{bc}, S_{ca} and switching functions related to phase current S_{a}, S_{b}, S_{c}.

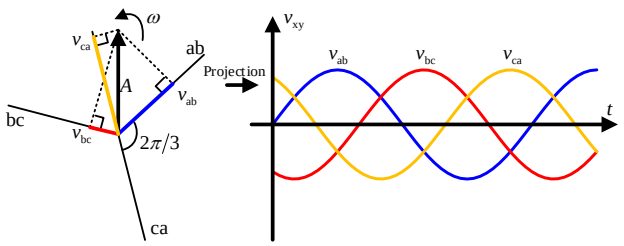

FIGURE 2. Formation of the line voltage via the rotating vector.

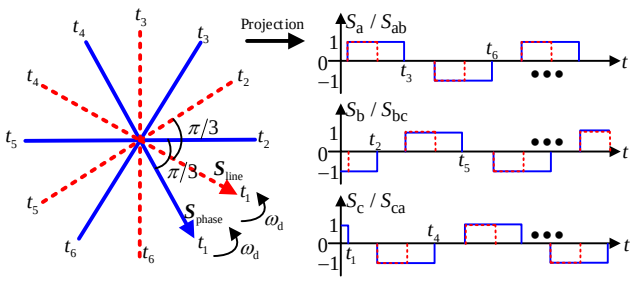

FIGURE 3. Formation of the line/phase switching function via the corresponding pulse rotating vector $\boldsymbol{S}_{\mathrm{line}}$ and $\boldsymbol{S}_{\mathrm{phase}}$.

represented by ω_{d} which equals ω_0 in the steady state. Therefore, the vector revolves at the speed of ω_0 in the steady state and ω_{d} in dynamics which is obviously time-varying. As the vector rotates at $\pi/3$, a pulse is triggered.

Further, the switching function waveforms shown in Fig. 1 can also be curved using frequency time-varying rotating vectors. The dynamics of the alternating square wave signal $S_{\mathrm{ab}}/S_{\mathrm{bc}}/S_{\mathrm{ca}}$ (or $S_{\mathrm{a}}/S_{\mathrm{b}}/S_{\mathrm{c}}$) are uniquely dependent on frequency of the firing pulse ω_{d}. Besides, any two switching functions among $S_{\mathrm{ab/bc/ca}}$ (or $S_{\mathrm{a/b/c}}$) differ in phase by $2\pi/3$ with each other. Therefore, $S_{\mathrm{ab/bc/ca}}$ and $S_{\mathrm{a/b/c}}$ can be integrated to form the rotating vector $\boldsymbol{S}_{\mathrm{line}}$ and $\boldsymbol{S}_{\mathrm{phase}}$, respectively, as (7) shows.

$$\begin{cases} \boldsymbol{S}_{\mathrm{line}} = S_{\mathrm{ab}} + S_{\mathrm{bc}} e^{j(2\pi/3)} + S_{\mathrm{ca}} e^{j(4\pi/3)} \\ \boldsymbol{S}_{\mathrm{phase}} = S_{\mathrm{a}} + S_{\mathrm{b}} e^{j(2\pi/3)} + S_{\mathrm{c}} e^{j(4\pi/3)} \end{cases} \quad (77)$$

ω_{d} in (6) implies time interval (t_{n}-$t_{\mathrm{n-1}}$) between adjacent firing pulses is varying, as shown in (6). Consequently, the dynamics of $\boldsymbol{S}_{\mathrm{line}}$ and $\boldsymbol{S}_{\mathrm{phase}}$ determined by ω_{d}, can also be expressed using time-varying frequency rotating vectors.

According to (2), the AC current is generated from the firing pulse and the DC current. Now that the firing pulse pattern has

time-varying frequency, the AC current naturally possesses the time-varying A/F as the DC current changes.

D. VALUES OF TIME-VARYING AMPLITUDE/FREQUENCY ROTATING VECTORS DESCRIPTION TO THE AC SIGNALS DYNAMICS

In terms of AC/DC conversion, the AC signals include the AC voltage, the firing pulse pattern, and the AC current, as (1)(2) and Fig. 1 show. The preceding paragraphs demonstrate their nature of time-varying A/F. As a result, the dynamics can all be described using rotating vectors with time-varying A/F. The values of employing rotating vectors to describe the dynamics of AC signals lie in two aspects as follows.

Firstly, the time-varying A/F rotating vector description is in accordance with the signal generation principle. As we can see in Fig. 2, time-varying A/F AC voltage rotating vector projects to generate AC voltage waveform. In Fig. 4(a), it displays AC voltage on the time axis and on the phase axis respectively. We can see that in steady-state condition, the AC voltage on the time axis and on the phase axis coincide with each other in steady-state conditions (before 1 s) since the frequency is constant, which represents the times AC voltage signal repeats its variation per second. However, the AC voltages on the time-axis and on the phase-axis do not coincide with each other in grid dynamic condition, since the AC voltage is no longer periodic signal, and the time-varying frequency (angular velocity of AC voltage rotating vector in Fig. 2) shortens (or lengths) the alternating time interval corresponding to the phase interval of 2π.

Apart from AC voltage, Fig. 4(b) displays how firing pulse is generated on the time axis and on the phase axis. Equidistant firing control means that the phase interval of adjacent pulses are is $\pi/3$. In steady-state conditions, AC voltage tracked by PLL is a sinusoidal wave, and the firing angle command remains constant, and thus the time interval of adjacent pulses remains constant, corresponding to the constant phase interval. Specifically, firing pulses originated from u_{ac} keep constant time interval as well as constant phase interval in steady-state condition, as shown in dotted blue line and solid red line of Fig. 4(b). Therefore, the firing pulse pattern in steady-state conditions is a periodic signal with a fixed frequency. However, in a practical dynamic process, the dynamics of AC voltage and firing angle command lead to the varying time interval between firing pulses corresponding to constant phase interval, as shown in the solid blue and red line of Fig. 4(b).Considering that AC current is originated from the firing pulse signal in (2), AC current is thus not the periodic signal during dynamics. It's worth mentioned that the so-called frequency is naturally generated via controller regulation instead of the definition from the periodic signal repeating times per second. The variation nature of AC signals with the time-varying A/F of practical AC signals has not been sufficiently recognized, which needs to be focused [15], [17].

Secondly, the rotating vector is a geometric tool to describe the dynamics of AC signal, and thus it can intuitively show

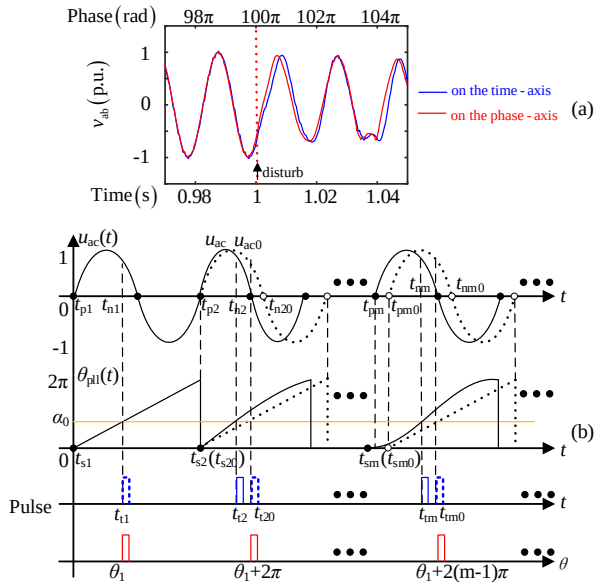

FIGURE 4. Constant and time-varying A/F for describing AC signals. (a) AC voltage on the time/phase axis. (b) firing pulse on the time/phase axis.

how AC signal varies. Specifically, take AC voltage in Fig. 4(a) for example, the length of AC voltage rotating vector explains the envelope of AC voltage, and the angular velocity of AC voltage rotating vector explains why the time interval of zero crossings varies. How AC/DC voltage and current converse can then be clarified to help readers intuitively understand the feature of the conversion between AC/DC voltage and current in LCC main circuits, which is essential to analyze grid dynamic problems. Therefore, in the following section, we will utilize the time-varying A/F rotating vectors to demonstrate the mechanism of conversion between AC/DC voltage and current in LCC main circuits.

III. MECHANISM OF CONVERSION BETWEEN AC/DC VOLTAGE AND CURRENT IN LCC MAIN CIRCUITS

This section aims to elaborate the mechanism of conversion between AC/DC voltage and current. As far as concerned, the switching function description of (1)(2) cannot reveal the feature of AC/DC signals and AC/DC conversion in grid dynamics. The utilization of time-varying A/F rotating vectors unveils the underlying conversion mechanism. First, the instantaneous AC voltage is decomposed to obtain two components of the DC voltage based on the idea of vector decomposition. Subsequently, the conversion mechanism for AC/DC voltage is described using the rotating vectors. Next, the DC/AC current conversion is described by the time-varying A/F rotating vector. Furthermore, the physical concept of active/reactive power is revealed based on the recognition of proposed AC/DC conversion mechanism, using rotating vectors to elucidate how power emerges from the voltage and current. Given the pivotal role of power exchange in grid dynamic analysis, this part aims to expand the value of the proposed AC/DC conversion mechanism. Finally, the

research idea is claimed unchanged even if the commutation process exists.

A. MECHANISM OF AC VOLTAGE AND FIRING PULSE FORMING DC VOLTAGE USING TIME-VARYING AMPLITUDE/FREQUENCY ROTATING VECTORS IGNORING THE COMMUTATION PROCESS

1) DECOMPOSITION OF AC VOLTAGE TO OBTAIN DC VOLTAGE BASED ON VECTORS DECOMPOSITION

The rotating vectors $\boldsymbol{v}_{\text{line}}$ and $\boldsymbol{S}_{\text{line}}$ which are formed by $v_{\text{ab/bc/ca}}$ and $S_{\text{ab/bc/ca}}$ respectively, can be utilized to describe the DC voltage according to (1). Considering that the DC voltage arises from the multiplication of $v_{\text{ab/bc/ca}}$ and corresponding $S_{\text{ab/bc/ca}}$, by the tool of rotating vectors, the DC voltage is also the result of product of $\boldsymbol{v}_{\text{line}}$ and $\boldsymbol{S}_{\text{line}}$, as (8) shows

$$v_{\text{d}} = \boldsymbol{v}_{\text{line}} \bullet \boldsymbol{S}_{\text{line}} \tag{8}$$

However, the rotating vector $\boldsymbol{S}_{\text{line}}$ rotates at a discrete speed, owing to the non-continuous variation of $S_{\text{ab/bc/ca}}$, determines that (8) cannot be directly manipulated based on regular rule of dot product. Therefore, the idea of vector operation is invoked to deal with the original expression of (1), so as to finally understand the AC/DC voltage conversion process using the rotating vectors.

As far as concerned, $\boldsymbol{v}_{\text{line}}$ can be decomposed into two components: $\boldsymbol{v}_{\text{p}}$ which is in phase with $\boldsymbol{S}_{\text{line}}$, and $\boldsymbol{v}_{\text{q}}$ which is orthogonal to $\boldsymbol{S}_{\text{line}}$, as shown in Fig. 5 (a). Considering that $v_{\text{ab/bc/ca}}$ are projections of $\boldsymbol{v}_{\text{line}}$ on ab, bc, and ca axes, $v_{\text{ab/bc/ca}}$ can be obtained by the sum of projections of $\boldsymbol{v}_{\text{p}}$ and $\boldsymbol{v}_{\text{q}}$ on ab, bc, and ca axes, respectively, so

$$v_{\text{xy}} = v_{\text{xy\_p}} + v_{\text{xy\_q}} \left(\text{xy} = \text{ab}, \text{bc}, \text{ca}\right) \tag{9}$$

where $v_{\text{ab\_p}}$, $v_{\text{bc\_p}}$, $v_{\text{ca\_p}}$ are the projections of $\boldsymbol{v}_{\text{p}}$ on ab, bc, and ca axes, whereas $v_{\text{ab\_q}}$, $v_{\text{bc\_q}}$, $v_{\text{ca\_q}}$ correspond to $\boldsymbol{v}_{\text{q}}$, as shown in Fig. 5 (b).

Combining (1)(9), DC voltage can then be expressed as

$$\begin{aligned} v_{\text{d}} &= v_{\text{dp}} + v_{\text{dq}} \\ v_{\text{dp}} &= v_{\text{ab\_p}} S_{\text{ab}} + v_{\text{bc\_p}} S_{\text{bc}} + v_{\text{ca\_p}} S_{\text{ca}} \\ v_{\text{dq}} &= v_{\text{ab\_q}} S_{\text{ab}} + v_{\text{bc\_q}} S_{\text{bc}} + v_{\text{ca\_q}} S_{\text{ca}} \end{aligned} \tag{10}$$

where $v_{\text{xy\_p}}$ is in phase with S_{xy} and $v_{\text{xy\_q}}$ is orthogonal to S_{xy} because of the phase relationship between $\boldsymbol{v}_{\text{p}}$, $\boldsymbol{v}_{\text{q}}$, and $\boldsymbol{S}_{\text{line}}$. This decomposition towards (1) is pivotal, as the original switching function (1) fails to reveal AC/DC conversion's feature in grid dynamics, while the idea of decomposition tries to give more detail explaining the AC/DC conversion's feature about how AC/DC signals converse.

Fig. 1 (a) implies that only one component of $S_{\text{ab/bc/ca}}$ is nonzero at any time, so the DC voltage can be simplified as

$$v_{\text{d}} = v_{\text{xy}} S_{\text{xy}} = v_{\text{dp}} + v_{\text{dq}}, \quad v_{\text{dp/q}} = v_{\text{xy\_p/q}} S_{\text{xy}} \tag{11}$$

That nonzero S_{xy} component is multiplied by v_{xy} to obtain the DC voltage, as shown by the red curve in Fig. 6 (a), where the firing angle α is the phase difference between S_{xy} and v_{xy}.

v_{dp} in (11) is equivalent to the green curve in Fig. 6 (b1). v_{xy} multiplies its amplitude by cosα and shifts to the right by α to form $v_{\text{xy\_p}}$ which is in phase with S_{xy}. Thus, $v_{\text{xy\_p}}$ multiplies S_{xy}

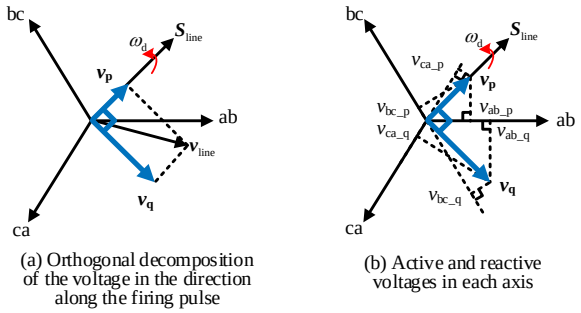

(a) Orthogonal decomposition of the voltage in the direction along the firing pulse

(b) Active and reactive voltages in each axis

FIGURE 5. Two voltage components which are in-phase and orthogonal to the firing pulse and their projection onto the stationary coordinate system.

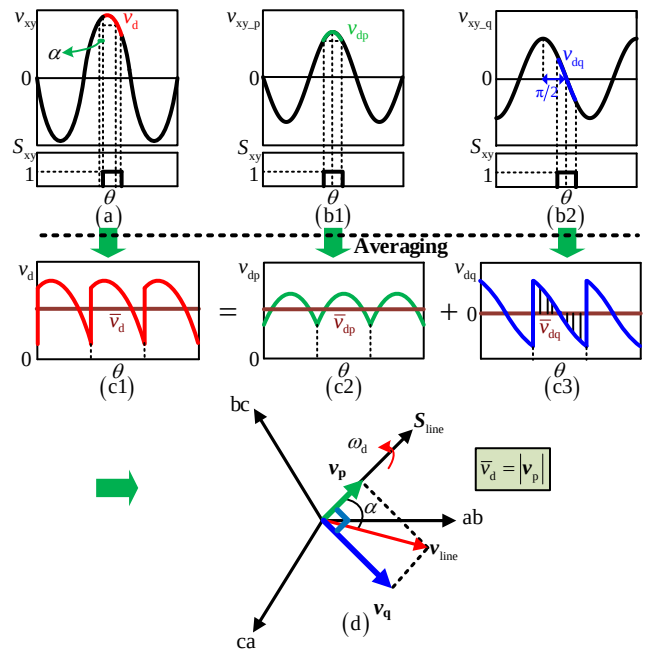

FIGURE 6. Mechanism of conversion between AC/DC voltage using rotating vectors. (a) Formation of the DC voltage. (b) Decomposition of the DC voltage into two components. (c) DC voltage and its two components on average. (d) DC voltage generation as the length of the projection of v_{line} on S_{line}.

to be v_{dp} (the green curve) in Fig. 6 (b1). Similarly, v_{dq} of (11) is equivalent to the blue curve in Fig. 6 (b2). v_{xy} multiplies its amplitude by sinα and shifts to the left by (π/2-α) to form $v_{\text{xy\_q}}$ which is orthogonal to S_{xy}. Finally, $v_{\text{xy\_q}}$ multiplies S_{xy} to be v_{dq} (the blue curve) in Fig. 6 (b2).

2) MECHANISM OF CONVERSION BETWEEN AC AND DC VOLTAGE USING TIME-VARYING AMPLITUDE/FREQUENCY ROTATING VECTORS

Considering that the controller's bandwidth slower than the switch dynamics, research to the controller-dominated grid dynamic problem is appropriate to disregard firing pulse interval dynamics. Then, the average DC voltage can reflect the DC voltage dynamics, where the A/F of the line voltage remains approximately constant within the adjacent firing pulses interval, shown as the brown curve in Fig. 6 (c1). Similarly, v_{dp} and v_{dq} in Fig. 6 (b1)(b2) are averaged to form the brown curve in Fig. 6 (c2)(c3), respectively. It is clear that

the average of v_{dp} is greater than zero, whereas the average of v_{dq} is zero because the midpoint of the blue curve in Fig. 6 (c3) crosses the zero axis causing the integral of v_{dq} within the pulse interval to be zero, which means

$$\bar{v}_d = \bar{v}_{dp} \left(\bar{v}_{dq} = 0 \right) \quad (12\text{~~12~~})$$

Such a graphical expression of the DC voltage can then be described using rotating vectors. According to (12), the average DC voltage is determined by the average of v_{dp} which is physically understood as the dot product of $\boldsymbol{v}_p$ and $\boldsymbol{S}_{line}$, so that (8) can be revised as

$$\bar{v}_d = \boldsymbol{v}_{line} \bullet \boldsymbol{S}_{line} = \boldsymbol{v}_p \bullet \boldsymbol{S}_{line} = V_{line} \cos\alpha \quad (13\text{~~13~~})$$

(13) geometrically reveals the DC voltage as the length of $\boldsymbol{v}_p$ formed by the projection of $\boldsymbol{v}_{line}$ on $\boldsymbol{S}_{line}$, as shown in Fig. 6 (d). Apparently, compared to (1), (13) reveals the conversion's feature of time-varying AC signals' projection to form DC voltage in the grid dynamics, laying the groundwork for further research on grid dynamics analysis.

B. MECHANISM OF DC CURRENT AND FIRING PULSE FORMING AC CURRENT USING TIME-VARYING AMPLITUDE/FREQUENCY ROTATING VECTORS IGNORING THE COMMUTATION PROCESS

Based on (2), the phase AC current i_a, i_b, i_c collectively form the phase current rotating vector $\boldsymbol{i}_{phase}$. The waveforms of i_a on the time/phase axis are schemed as an example in Fig. 7(a), i_b, i_c follow the similar generation process as i_a does. In Fig. 7(a), t_n represents the time of pulse triggered, as indicated in Fig. 3, and the phase interval of the AC current square-wave remains $2\pi/3$ due to equidistant firing control. In steady-state condition, the fixed frequency of AC current implies the time interval of AC current square-wave is constant of 6.6ms as shown in dotted line. However, during grid dynamics, due to the dynamics of PLL and firing angle command, the time interval of the adjacent pulses is varying, as shown in solid line. And the amplitude of i_a, i_b, i_c is changing as DC current varies in grid dynamics. Specifically, combing (2)(7), the i_a, i_b, i_c can form the rotating vector $\boldsymbol{i}_{phase}$, as (14) shows.

$$\boldsymbol{i}_{phase} = i_d \bullet \boldsymbol{S}_{phase} \quad (14\text{~~14~~})$$

DC current proportionally modulates the AC current's amplitude, while the AC current's frequency changes in accordance with that of $\boldsymbol{S}_{phase}$ which equals to ω_d in (6), as shown in Fig. 7 (b). Based on averaging, the amplitude and frequency of AC current is as (15) shows.

$$I = 2\sqrt{3} i_d / \pi, \omega_i = \omega_d \quad (15\text{~~15~~})$$

(15) clarifies how AC current is formed, deriving from the pulse vector's amplitude modulation.

Apparently, compared to (2), the rotating vector naturally reveal the AC current's state of amplitude and frequency during grid dynamics, which are hidden behind the AC instantaneous value as (2) declares. Especially in Fig. 7(a), the constant phase interval of square-wave AC current leads to corresponding time interval, which is constant in steady state and varying in dynamics. The reason to explain such result is

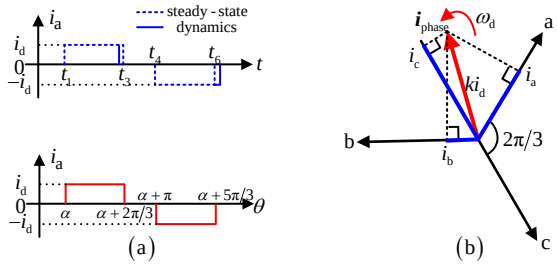

FIGURE 7. Mechanism of conversion between AC/DC current using rotating vectors. (a) AC current i_a schemed on the time/phase axis to show it's A/F. (b) Formation of AC current via the rotating vector.

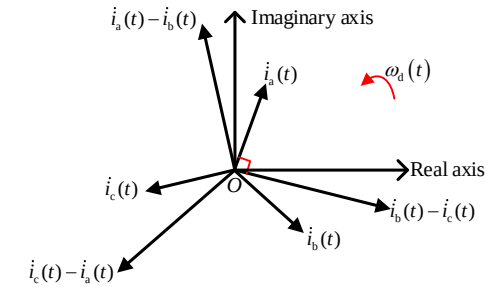

FIGURE 8. Phasor diagram of time-varying amplitude/frequency rotating phasor corresponding to AC phase current.

the time-varying AC current frequency reflected in the angular velocity of the rotating vector in Fig. 7(b). Due to the fact that vector description is in accordance with the AC current generation principle, it naturally reveals how DC current evolves to AC current regardless the condition of steady-state or dynamics. Therefore, the rotating vector leads to an application of a geometric description of phasor with time-varying amplitude/frequency, such a geometric description with 'phasor diagram' will be of benefit to understanding the grid dynamics [21]. The dynamics of the AC instantaneous value can be drawn using time-varying amplitude/frequency rotating phasors, as shown in Fig. 8. In the past, traditional phasor can only be used to describe periodic AC instantaneous value signal at fixed frequency in a single-phase sinusoidal steady-state circuit [18], [22]. Now we extend the concept of "phasor diagram" to "rotating phasor diagram", so that for AC instantaneous value signal in practical grid dynamics, even if it is non-periodic during grid dynamics, it can also be depicted with time-varying amplitude/frequency [21], [24]. It is hoped that this advancement can enable researchers understand the grid dynamic as easily as they understand the system steady state via the traditional "phasor method".

Next, another application in understanding the concept of power during grid dynamics is briefly described.

C. PHYSICAL CONCEPT OF ACTIVE/REACTIVE POWER BASED ON AC/DC VOLTAGE AND CURRENT CONVERSION MECHANISM

Considering that power transmission is crucial to the grid and the power exchange greatly influences grid dynamics stability mechanism, the clarification of the physical concept of the

active/reactive power is paramount, which helps us understand how power is generated. However, the existing works predominantly address the active/reactive power in steady state condition, thereby limiting our understanding of power in grid dynamics [24]. Consequently, elucidating the physical concept of active/reactive power in grid dynamics is imperative and is presented based on the aforementioned voltage/current conversion mechanism as follows.

The challenge in understanding the physical concept of the active/reactive power lies in the description of AC signals, especially the AC current in square wave. The work in [24] has briefly illustrated how active/reactive power is originated from the time-varying A/F of AC voltage and AC current. Therefore, the main task here is to combine the actual voltage/current signals in the LCC-HVDC station to form the physical concept of the active/reactive power via time-varying rotating vectors.

On one hand, the physical concept of the active power is presented as follows. Active power flows on the DC line, where LCC-HVDC transmits power to the loads. Then, considering that the line current can be obtained by multiplying the DC current with $S_{ab/bc/ca}$, so that together with (1), DC side power is derived as

$$P_d = v_d i_d = v_{ab} i_{ab} + v_{bc} i_{bc} + v_{ca} i_{ca} \quad (16\text{~~16~~})$$

According to the decomposition of DC voltage in (10) and feature of v_{dp} greater than zero on average, v_{dq} equal to zero on average shown in Fig. 4, the active power satisfies that

$$P_d = P_{dp} + P_{dq}, P_{dp} = v_{dp} i_d, P_{dq} = v_{dq} i_d \quad (17\text{~~17~~})$$

$$\bar{P}_d = \bar{P}_{dp} \left(\bar{P}_{dq} = 0 \right) \quad (18\text{~~18~~})$$

Consequently, when we measure the effect of active power doing work, only part of (17) steadily supplies the energy which is characterized as P_{dp}. Given that v_{dp} is the projection of $\boldsymbol{v}_{line}$ on $\boldsymbol{S}_{line}$, whereas $\boldsymbol{S}_{line}$ combines with i_d to form $\boldsymbol{i}_{line}$, thus, the active power is featured as the dot product of $\boldsymbol{v}_p$ and $\boldsymbol{i}_{line}$ in dynamic process, physically flowing at the DC side.

On the other hand, the physical concept of the reactive power is presented as follows. Reactive power describes part of the instantaneous power in the AC system characterized in not doing work externally in overall. The instantaneous power of three-phase AC system is described as (19) in [24]

$$S_{AC} = v_a i_a + v_b i_b + v_c i_c \quad (19\text{~~19~~})$$

Based on the AC-DC relationship which is described using switching functions [20], (19) satisfies that

$$v_d i_d = v_a i_a + v_b i_b + v_c i_c \quad (20\text{~~20~~})$$

Combining (16), (19) with (20) yields

$$S_{AC} = v_{ab} i_{ab} + v_{bc} i_{bc} + v_{ca} i_{ca} \quad (21\text{~~21~~})$$

The instantaneous power at the AC side S_{AC} follows the same decomposition rule shown in (17)-(18). Hence, the part of (21) which doesn't do work externally in overall is characterized as P_{dq} whose value is zero. The feature of the reactive power corresponds to S_q which is given by (10), (16) and (17)

$$S_q = v_{dq} i_d = v_{ab\_q} i_{ab} + v_{bc\_q} i_{bc} + v_{ca\_q} i_{ca} = \boldsymbol{v}_q \bullet \boldsymbol{i}_{xy} \quad (22\text{~~22~~})$$

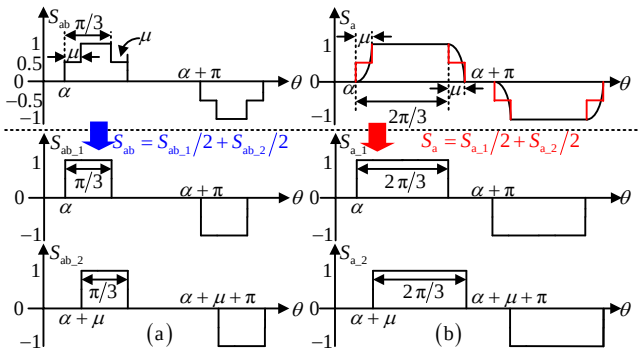

FIGURE 9. AC/DC conversion with the commutation process. (a) Voltage conversion idea with the commutation process. (b) Current conversion idea with the commutation process.

Similarly, based on the representation of v_d as a vector projection, S_q can then be understood as the dot product of $\boldsymbol{v}_q$ and $\boldsymbol{i}_{line}$, which is averaged to be zero, as shown in (18). Physically the reactive power is indicated to circulate in AC system, which does not do work externally in overall. Hence the physical concept revealing the power formation is rooted in the geometric approach of rotating vectors. Based on the above explanation, we can see that the active/reactive power in grid dynamics is not defined according to the steady-state result as it used to be recognized, but naturally separated [25]-[26]. The rational understanding on active/reactive power serves as the basis for system dynamic analysis.

D. RESEARCH IDEA OF THE CONVERSION MECHANISM BETWEEN AC AND DC ELECTRICAL VARIABLES WITH THE COMMUTATION PROCESS

AC current does not vary abruptly during the commutating process, resulting that switching functions in Fig. 1 vary with the commutation angle μ, as shown in Fig. 9.

Concerning voltage conversion, S_{ab} in (1) is decomposed into the average of two waveforms in Fig. 9(a). S_{ab_1} and S_{ab_2} are the waveforms in the case without the commutation process, respectively. Thus, the DC voltage is derived as

$$\begin{aligned} v_d &= \left(v_{d1} + v_{d2} \right)/2 \\ v_{d1} &= v_{ab} S_{ab\_1} + v_{bc} S_{bc\_1} + v_{ca} S_{ca\_1} = v_{d1p} + v_{d1q} \\ v_{d2} &= v_{ab} S_{ab\_2} + v_{bc} S_{bc\_2} + v_{ca} S_{ca\_2} = v_{d2p} + v_{d2q} \end{aligned} \quad (23\text{~~23~~})$$

So the DC voltage can be described based on components v_{d1} and v_{d2} in two cases without commutation process. Specifically, v_{d1} and v_{d2} both represent projections of $\boldsymbol{v}_{line}$ on $\boldsymbol{S}_{line}$ based on the knowledge in previous parts. However, the phase difference between $\boldsymbol{v}_{line}$ and $\boldsymbol{S}_{line}$ for v_{d1} is the firing angle α, whereas for v_{d2} it is $(\alpha+\mu)$. Thus, the DC voltage is the average of two sets of vector projections in equivalent cases without commutation process.

Regarding current conversion, S_a in (2) is decomposed into the average of S_{a_1} and S_{a_2}, as shown in Fig. 9(b). S_{a_2} lags behind S_{a_1} by μ. Thus, $\boldsymbol{S}_{phase}$ is the combination of two pulse rotating vectors whose amplitude/frequency follow the same pattern as claimed in (15).

Finally, the physical concept of power revealing how active/reactive power generate, follows the same research idea. v_{xy} can be decomposed into four parts: $v_{xy\_1\_p}$, $v_{xy\_2\_p}$, $v_{xy\_1\_q}$, and $v_{xy\_2\_q}$, where $v_{xy\_1\_p}$ ($v_{xy\_2\_p}$) is in-phase with S_{xy_1} (S_{xy_2}), and $v_{xy\_1\_q}$ ($v_{xy\_2\_q}$) is orthogonal to S_{xy_1} (S_{xy_2}) according to the rule of (9)-(10). And S_{xy_1} (S_{xy_2}) is generated based on Fig. 9(a). Therefore the power formation is still studied in a way similar to (17)-(18), as shown in (24). Among them, the average of the 'orthogonal' components is zero reflecting the feature of the reactive power, while the average of the 'in-phase' components indicates the active power. Thus, the research idea remains unchanged even if the commutation process exists.

$$P_{\mathrm{d}} = \left(\underbrace{P_{\mathrm{d1p}} + P_{\mathrm{d1q}}}_{P_{\mathrm{d1}}} + \underbrace{P_{\mathrm{d2p}} + P_{\mathrm{d2q}}}_{P_{\mathrm{d2}}} \right) \Big/ 2$$

$$P_{\mathrm{d1p}} = \sum v_{\mathrm{xy\_1\_p}} S_{\mathrm{xy\_1}} i_{\mathrm{d}}, P_{\mathrm{d1q}} = \sum v_{\mathrm{xy\_1\_q}} S_{\mathrm{xy\_1}} i_{\mathrm{d}} \quad (2424)$$

$$P_{\mathrm{d2p}} = \sum v_{\mathrm{xy\_2\_p}} S_{\mathrm{xy\_2}} i_{\mathrm{d}}, P_{\mathrm{d2q}} = \sum v_{\mathrm{xy\_2\_q}} S_{\mathrm{xy\_2}} i_{\mathrm{d}}$$

In the end of the Section, it is essential to acknowledge the limitation of the proposed mechanism in terms of use scope. Firstly, the description based on the rotating vectors means the switching function $S_{\mathrm{ab/bc/ca}}$ (or $S_{\mathrm{a/b/c}}$) shares the same amplitude/frequency and only different in phase by $2\pi/3$, so that if the commutation failure occurs at the converter station, where the switch valve is not functioning normally, this mechanism is no longer valid to this station. Besides, the rotating vector is used to averagely portray the AC signals dynamics, meaning the dynamics of AC signals within the pulse interval is ignored. Considering that the timescale of switch dynamics within the pulse interval is 3.3ms, the work is applicable to the study of dynamics on timescales slower than switch dynamics. In fact, this consideration meets the needs of grid dynamic analysis. As the bandwidth of the converter station control is slower than the timescale of switch dynamics, so the widely-focused grid dynamics dominated by the controller regulation are slower than switch dynamics. Therefore, the omission of AC signal dynamics faster than switch dynamics does not hinder the recognition of the value of this work. After all, the work in this paper serves to help analyze such grid dynamic problems, rather than a clarification of AC/DC conversion about general signal analysis.

IV. CASE STUDY

This section first shows the time-varying nature of AC voltage and current A/F, and then validates the proposed AC/DC conversion mechanism, including the power generation, finally present proposed work's benefit to research grid dynamics. Considering that the proposed work is for researching practical grid dynamics, a multi-devices system is chosen as a study system, instead of CIGRE benchmark with only converter station. The study system contains an SG unit, a grid-tied voltage source converter (VSC), a two-terminal LCC-HVDC, as shown in Fig. 10. The simulation model is built in PSCAD/EMTDC, where key parameters are given in

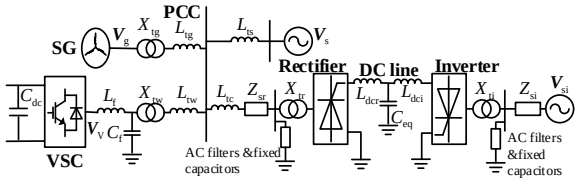

FIGURE 10. Circuit structure of the study system.

TABLE I
PARAMETERS IN THE SIMULATION CASE

Parameters		Value	Parameters		Value
Rated Value	S_{b}(MVA)	500	VSC Control	$k_{\mathrm{pdc}}/k_{\mathrm{idc}}$	5/50
	V_{b}(kV)	345			
	ω_{b}(rad/s)	100π		$k_{\mathrm{pV}}/k_{\mathrm{iV}}$	1/5
	V_{dcb}(kV)	250			
Trans-former	X_{tg}/ X_{tw}/X_{tr}/ X_{ti} (p.u.)	0.08/0.06/ 0.08/0.08		$k_{\mathrm{ppll}}/k_{\mathrm{ipll}}$	200/20000
				$k_{\mathrm{pi}}/k_{\mathrm{ii}}$	6/200
VSC Circuit	C_{dc}(F)	0.078	LCC control	$k_{\mathrm{pi}}/k_{\mathrm{ii}}$	0.80/1.96
	C_{f}(uF)	200		$k_{\mathrm{ppll}}/k_{\mathrm{ipll}}$ (Rev/ Inv)	10/50
	L_{f}(H)	0.003			
Line	L_{tg}/ L_{tw}/L_{tc}/ L_{ts}(mH)	23.2/20/ 10/200		$k_{\mathrm{pv}}/k_{\mathrm{iv}}$	0.75/18.52

Table I. Parameters of DC line, filters, compensators, Z_{sr} and Z_{si} are all given according to the CIGRE benchmark [27].

A. AC-DC CONVERSION MECHANISM VERIFICATION

Case: the DC voltage reference of the VSC changes from 1 p.u. to 1.05 p.u. at t=1 s.

First, sending-end's AC voltage v_{a} as well as its amplitude and frequency, the AC current i_{a} as well as its envelope (amplitude) and frequency are displayed in Fig. 11 and Fig. 12. AC voltage/AC current are verified to have time-varying A/F. Apparently, AC voltage/AC current are no longer periodic signals as they are in steady-state condition, which means the traditional concept of frequency about the periodic signal repeating its variation per second cannot reveal the feature of distortion of AC voltage/AC current instantaneous values during dynamics. So that the proposed work via the length/angular velocity of rotating vector is motivated to physically describe the A/F dynamics of AC voltage/AC current for AC/DC conversion mechanism research [19].

Second, the rectifier station's DC voltage v_{d} as well as its two separate components v_{d1} and v_{d2}, and (v_{d1} + v_{d2})/2 are shown in Fig. 13. Here v_{d1} and v_{d2} are defined based on (23). According to Fig. 13, the original DC voltage indeed equals to (v_{d1} + v_{d2})/2 as (23) demonstrates. v_{d1} and v_{d2} are decomposed into $v_{\mathrm{d1p/q}}$ and $v_{\mathrm{d2p/q}}$ respectively. It's clear that v_{d1p} and v_{d2p} are both greater than zero, indicating that their average values are always greater than zero. In contrast, the integral of v_{d1q} and v_{d2q} within the adjacent firing pulse interval are both zero, indicating that their average values are equal to zero. Therefore, the average DC voltage is generated from the average of (v_{d1p} + v_{d2p})/2. Here v_{d1p} and v_{d2p} refer to two cases of the projection of $\boldsymbol{v}_{\mathrm{line}}$ on $\boldsymbol{S}_{\mathrm{line}}$ without commutation process.

Third, in Fig. 12 (a)(b), the AC current is verified indeed

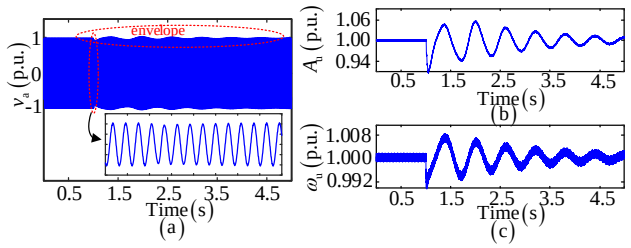

FIGURE 11. AC voltage with time-varying A/F. (a) AC voltage. (b) AC voltage amplitude. (c) AC voltage frequency.

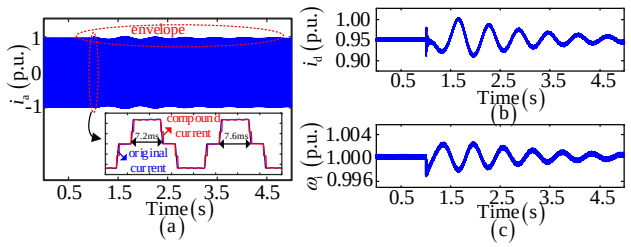

FIGURE 12. AC current with time-varying A/F. (a) AC current and compound current based on Fig. 9 (b). (b) DC current. (c) AC current frequency.

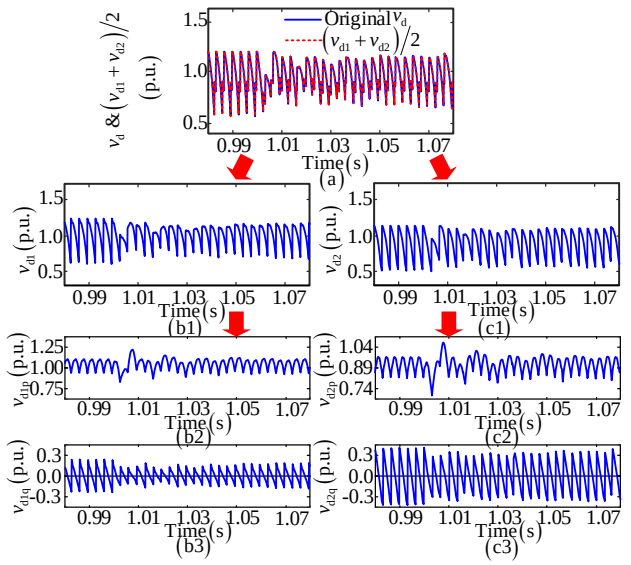

FIGURE 13. DC voltage formation process. (a) DC voltage and $(v_{d1}+v_{d2})/2$. (b) v_{d1} and its decomposed components. (c) v_{d2} and its decomposed components.

generated from a compound of two pulse currents based on Fig. 9 (b). The AC current envelope representing its amplitude varies with the DC current, and its frequency leads to the change of the pulse width. Apparently, the A/F is the length/angular velocity of AC current rotating vector directly affected by the controller. Specially, the frequency here is different from the traditional concept 'frequency' from periodic signal, which represents the times of periodic signal repeating its variation per second.

B. VERIFICATIONS FOR PHYSICAL CONCEPT NATURE OF THE POWER

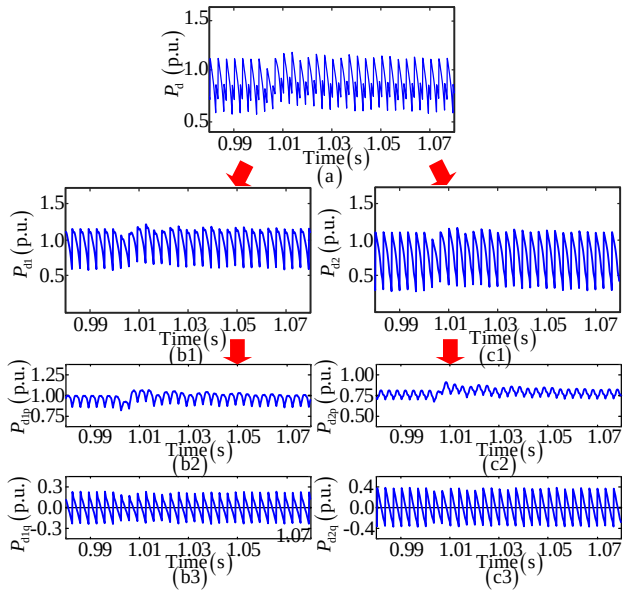

FIGURE 14. Physical concept of power. (a) DC side power. (b) P_{d1} and its decomposed components. (c) P_{d2} and its decomposed components.

The physical concept nature of the power aims to reveal how the active/reactive power is generated based on the voltage and current which follow the above conversion mechanism during grid dynamics.

The waveforms of DC side power when the commutation process is considered are displayed in Fig. 14. The power is determined by P_{d1} and P_{d2} according to (24), where P_{d1} and P_{d2} can be decomposed into its in-phase and orthogonal components respectively as (24) shows. We can see that the in-phase components shown in Fig. 14 (b2)(c2) are always greater than zero, whereas orthogonal components shown in Fig. 14 (b3)(c3) are alternating signals with an average of zero. Considering that the DC side power is equal to the instantaneous power at the AC side in (20), the nature of the active power at the AC side lies in the in-phase component of DC side power (P_{d1p} and P_{d2p}), which does work externally. Hence, the active power is consistent with the understanding of the dot product of $\boldsymbol{v}_p$ and $\boldsymbol{i}_{line}$ ($\boldsymbol{i}_{line}$ shares the same generation process with $\boldsymbol{i}_{phase}$) in Section III. On the other hand, the nature of the reactive power at the AC side lies in the orthogonal component of DC side power (P_{d1q} and P_{d2q}), where the dot product of $\boldsymbol{v}_q$ and $\boldsymbol{i}_{line}$ equaling zero in Section III implies that it doesn't do work externally and the reactive power is physically understood to circulate in the AC system.

C. PRELIMINARY UNDERSTANDINGS ON THE BENEFIT OF PROPOSED MECHANISM TO RESEARCH GRID DYNAMICS

In Section III, we have demonstrated that 1) proposed AC/DC conversion mechanism can be applied to develop time-varying A/F phasors; 2) proposed AC/DC conversion mechanism can be applied to reveal the physical concept of active/reactive power. Aspect 1 contributes to fostering an intuitive and geometric understanding on AC electrical variables' dynamics

which can benefit grid dynamic analysis as traditional "phasor diagram" does in sinusoidal steady-state circuits. Aspect 2 helps reveal how the active/reactive power is formed in actual grid dynamics. Given that the power propels the electrical variables' dynamic, the rational recognition of the active/reactive power's physical concept serves as the basis for analyzing grid dynamics.

Drawn from aspect 1 and 2, active/reactive power and AC current A/F can serve as input and output to form an excitation-response relationship, thereby facilitating further exploration of station characteristics during grid dynamics [28]-[29]. This marks the third benefit to grid dynamic analysis. In following paragraphs, we will introduce the features of AC current output and power input, underscoring the value of delving deeper into the characteristics of such converter stations.

First, the AC current A/F is characterized in changing simultaneously in a non-independent way during grid dynamics. As the thyristor can only control the switch on, the station directly controls the frequency of AC current [18], whereas the AC current amplitude changes passively with the DC current according to the proposed current conversion mechanism in LCC main circuits.

Fig. 15 (a1)(a2) display the amplitude/frequency dynamics of the rectifier station's output current, showcasing their non-independent variations. The AC current amplitude will change in the opposite trend as the AC current frequency due partially to the station's non-independent control. Considering that for rectifier station,

$$P = UI\cos\left(\theta_u - \int \omega_i dt\right) \qquad (25\text{~~25~~})$$

The opposite trend of AC current amplitude and frequency may have opposite effect on the active power. That is to say, the AC current amplitude will affect the active power, as shown in Fig. 15 (b), and then the active power will affect the AC current frequency regulation problem, which may be influenced due to A/F opposite effect on the active power. It is worth mentioned that frequency regulation problem is crucial especially in the present weak grid with high penetration renewables because the variation of the frequency matters in the grid. Therefore, although we don't analyze the specific device's characteristics, the feature of the AC current A/F changing in a non-independent way benefits to grid dynamic analysis for its remind to note the hidden impact on the frequency regulation problem from the amplitude factor.

Second, the inherent nature of the active/reactive power generated suggests simultaneous, non-independent changes. As clarified in Section III, power variation is intertwined with the dynamics of voltage and current, subject to non-independent control. (16) declares that the active power determines the DC current, and DC current is controlled to further affect the power factor [28]. Given that the active/reactive power are linked by the power factor, the reactive power varies passively with the active power under non-independent control.

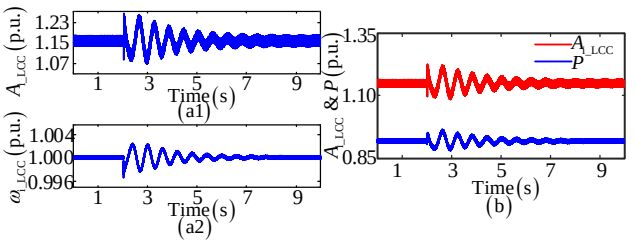

FIGURE 15. **AC current amplitude/frequency feature. (a) Amplitude and frequency of the rectifier station's output current to clarify their non-independent variations. (b) AC current amplitude and active power flowing via the rectifier station to highlight the amplitude factor's impact on the frequency regulation problem.**

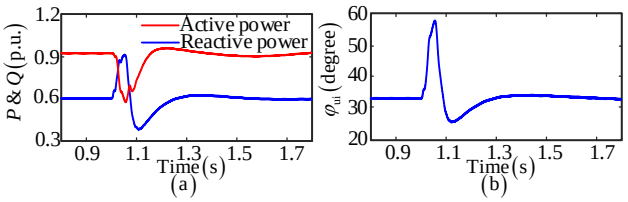

FIGURE 16. **Active/reactive power feature. (a) Active and reactive power of the rectifier station to display their non-independent variations. (b) Power factor angle to highlight the feature of power variations' impact on the voltage regulation problem.**

During grid dynamic process, the reactive power absorbed by the rectifier station decreases significantly, which will result in the reactive power surplus at the terminal increases with the sending-end voltage rising up, and that is also the mainstream explanation for the sending-end overvoltage [30]. According to Fig. 16 (a), the non-independent variation between the active and reactive power exists. And the derived power factor angle in Fig. 16 (b) presents the interaction between the active and reactive power under non-independent control. Considering that

$$Q = UI\sin\varphi_{ui} \qquad (26\text{~~26~~})$$

So that the voltage regulation is not only determined by reactive power variations, but also determined by the power factor under the feature of the active/reactive power interactions. Thus, the dynamics feature of active/reactive power will affect the power factor which may exert unknown effect on grid voltage dynamics stability.

The conversion mechanism between AC and DC variables in LCC main circuits as well as the derived features of AC current and power lays the groundwork for studying full characteristics of the station. Further, the study on station characteristics is critical to the grid dynamic analysis.

V. DISCUSSION

This section evaluates and synthesizes the contribution of the proposed work by comparison with traditional works.

Faced with controller-dominated grid dynamic problems including non-periodic AC signals, this paper transcends the traditional concept of frequency rooted in the framework of periodic signal, and recognizes the time-varying A/F characteristics of AC signals. Then, this paper utilizes time-varying A/F rotating vectors to portray the AC/DC conversion process in practical grid dynamics. However, the phasor-based

description is only applicable to sinusoidal steady-state circuits where AC signals are periodic [12], [22]. The harmonic description is also only applicable to the periodic steady-state condition [14], [23]. Moreover, the representation of AC instantaneous signal under switching function description lacks physical meaning, where the distortion of AC instantaneous values and discrete switching signal's variation are challenging to discern the features of grid dynamic operation.

Besides, the contribution of the proposed work lies in its three applications to benefit grid dynamic analysis as follows.

1) The proposed AC/DC conversion mechanism can be applied to develop time-varying A/F phasors which helps geometrically understand the grid dynamic process, surpassing the constraints of traditional "phasor method" which is only valid in sinusoidal steady-state condition where AC signals are periodic.

2) The proposed AC/DC conversion mechanism can be applied to reveal physical concept of active/reactive power, enhancing the understanding of power exchange processes during grid dynamics, but the traditional works just define power in grid dynamics from steady-state result [25]-[26].

3) The proposed AC/DC conversion mechanism can be applied to build the foundation for researching the device's active/reactive power-A/F characteristics. The focus on active/reactive power and A/F help draw attention to the potential negative effects of the unique control structure, offering insights not easily discernible via traditional works.

To sum up, the proposed vector-based AC/DC conversion mechanism in LCC main circuits, as well as its three applications, work together to build foundation for analyzing grid AC/DC dynamic problems dominated by the controller regulations in present power system.

VI. CONCLUSION

When faced with controller-dominated AC/DC interaction problems characterized by dynamics slower than switch dynamics excluding commutation failure, this paper utilizes time-varying A/F rotating vectors to depict the AC electrical variables during practical dynamics, thereby elucidating the conversion mechanism between AC and DC electrical variables in LCC main circuits

1) AC voltage, firing pulse pattern, and AC current participating in AC/DC conversion are generated naturally with the nature of time-varying A/F as non-periodic signal in grid dynamics.

2) Conversion mechanism between AC and DC electrical variables in LCC main circuits is clarified using time-varying A/F rotating vectors. The AC voltage rotating vector projects on the pulsed rotating vector to generate the DC voltage, while the DC current modulates the amplitude of the pulsed rotating vector to form the AC current rotating vector. The above conversion feature fills the gaps in explaining how and why AC/DC conversion is that during grid dynamics.

3) The proposed conversion mechanism, applied across three aspects, demonstrates its utility to benefit grid dynamic analysis. Firstly, the geometric approach is developed to help intuitively understand the grid dynamic process [21]. Secondly, physical concept of active/reactive power in system dynamics are revealed, enhancing the understanding of power exchange processes during grid dynamics. Further, link with future research on station characteristics is discussed. The features of the AC current and power are clarified to help build converter station's characteristics, where the state variables of active/reactive power and A/F remind us to note the related frequency and voltage regulation problems, as well as features' possibly adverse effect on them.

REFERENCES

[1] M. Li, "Characteristic analysis and operational control of large-scale hybrid UHV AC/DC power grids," *Power System Technology*, vol. 40, no. 4, pp. 985-991, Apr. 2016.
[2] X. Chen, H. Zhou, D. Wang, et al., "Study on transient overvoltage of Zhexi converter station of ±800kV DC power transmission project," *Power System Technology*, vol. 35, no. 3, pp. 22-27, Mar. 2012.
[3] G. Tzounas, R. Sipahi, and F. Milano, "Damping power ststem electromechanical oscillations using time delays," *IEEE Trans. Circuits Syst. Ⅰ, Reg. Papers*, vol. 68, no. 6, pp. 2725-2735, Jun. 2021.
[4] M. Zhang, X. Yuan, J. Hu, "Mechanism analysis of subsynchronous torsional interaction with PMSG-Based WTs and LCC-HVDC," *IEEE J. Emerging Sel. Topics Power Electron.*, vol. 9, no. 2, pp. 1708-1724, Apr. 2021.
[5] B. Gao, Y. Hu, R. Song, et al., "Impact of DFIG-based wind farm integration on subsynchronous torsional interaction between HVDC and thermal generators," *IET Gener., Transmiss. Distrib.*, vol. 12, no. 17, pp. 3913-3923, Sept. 2018.
[6] J. Sun, Y. Wang, P. Liu, et al., "Memristor-based neural network circuit with multimode generalization and differentiation on Pavlov associative memory," *IEEE Trans. Cybern.*, vol. 53, no. 5, pp. 3351-3362, May. 2023.
[7] J. Sun, Y. Wang, P. Liu, et al., "Memristor-based circuit design of PAD emotional space and its application in mood congruity," *IEEE Internet Things J.*, vol. 10, no. 18, pp. 16332-16342, Sep. 2023.
[8] W. Hammer, "Dynamic modeling of line and capacitor commutated converters for HVDC power transmission," Ph.D. dissertation, SFIT Zurich., 2003.
[9] M. Li, Z. Yu, T. Xu, et al., "Study of complex oscillation caused by renewable energy integration and its solution," *Power System Technology*, vol. 41, no. 4, pp. 1035-1042, Apr. 2017.
[10] G. Chen, M. Li, T. Xu, et al., "Practice and challenge of renewable energy development based on interconnected power grids," *Power System Technology*, vol. 41, no. 10, pp. 3095-3103, Oct. 2017.
[11] S. Huang, "Application of time-varying dynamics phasor theory in analysis of electric power system," Ph.D. dissertation, China Electric Power research Institute, Beijing, 2002.
[12] C. Liu, A. Bose, and P. Tian, "Modeling and analysis of HVDC converter by three-phase dynamics phasor," *IEEE Trans. Power Del.*, vol. 29, no. 1, pp. 3-12, Feb. 2014.
[13] S. C. D. Roy, "Characteristics of single- and multiple-frequency impedance matching networks," *IEEE Trans. Circuits Syst. Ⅱ, Exp. Briefs*, vol. 62, no. 3, pp. 222-225, Mar. 2015.
[14] A. Malkhandi, N. Senroy, and S. Mishra, "A dynamic model of impedance for online thevenin's equivalent estimation," *IEEE Trans. Circuits Syst. Ⅱ, Exp. Briefs*, vol. 69, no. 1, pp. 194-198, Jan. 2022.
[15] X. Yuan, S. Li, "An amplitude/frequency modulation based method of voltage source converter for power systems dynamic analysis in current control timescale," *Proc. of the CSEE*, vol. 40, no. 15, pp. 4732-4744, Aug. 2020.
[16] Z. Xu, *Dynamic Behavior Analysis of AC/DC Power System*. Beijing, BJ , CHINA: Machine, 2004, pp. 130-133.

[17] X. Gong, X. Yuan, J. Hu, et. al., "Modeling of VSC with active/reactive current excitation and internal voltage response for analyzing amplitude/frequency modulation dynamics of the grid," *CSEE J. Power Energy Syst.*, doi: 10.17775/CSEEJPES.2022.00560 .
[18] P. Kunder, *Power System Stability and Control*. New York, NY , USA: McGraw-Hill, 1994.
[19] D. Jovcic, N. Pahalawaththa, and M. Zavahir, " Analytical modelling of HVDC-HVAC systems," *IEEE Trans. Power Del*., vol. 14, no. 2, pp. 506-511, Apr. 1999.
[20] L. Hu, R. Yacamini, "Harmonic transfer through converters and HVDC links," *IEEE Trans. Power Electron*., vol. 7, no. 3, pp. 514-525, Jul. 1992.
[21] H. Yang, X. Yuan, "Analysis of inductor current and power in AC power system based on time-varying amplitude-frequency phasors sequence," *Proc. of the CSEE*, vol. 43, no. 11, pp.4261-4272, Jun. 2023.
[22] C. P. Steinmetz, "Complex quantities and their use in electrical engineering," *Proceedings of the International Electrical Congress*, 1893.
[23] V. Venkatasubramanian, "Tools for dynamic analysis of the general large power system using time-varying phasors," *International Journal of Electrical Power & Energy Systems*, vol. 16, no. 6, pp. 365-376, Dec. 1994.
[24] H. Yang, X. Yuan, "Physical concept understanding and mathematical calculation of active/reactive power in dynamic process of three-phase system under time-varying amplitude-frequency signals," *Proc. of the CSEE*, vol. 42, no. 2, pp. 548-558, Jan. 2022.
[25] B. Yin, Y. Chen, H. Deng, et. al., "Uniform mathematical description of instantaneous reactive power theory and conventional power theory and its physical meaning in α-β coordinates," *Trans. of China Elect. Soc.*, vol. 18, no. 5, pp. 42-45+58, Oct. 2003.
[26] J. Liu and Z. Wang, "Uniform mathematical description of instantaneous reactive power theory and conventional power theory and its physical meaning," *Trans. of China Elect. Soc.*, vol. 13, no. 6, pp. 6-12, Dec. 1998.
[27] M. Szechtman, T. Wess, C. V. Thio, "First benchmark model for HVDC system studies," *CIGRE Committee*, *Electra*, vol. 135, no. 4, pp. 54-73, 1991.
[28] J. Lu, X. Yuan, J. Hu, et al., "Motion equation modeling of LCC-HVDC stations for analyzing DC and AC network interactions," *IEEE Trans. Power Delivery*, vol. 35, no. 3, pp. 1563-1574, Jun. 2020.
[29] J. Huang, X. Yuan, S. Wang, "Power-imbalance stimulation and internal-voltage response relationships based modeling method of PE-interfaced devices in dc voltage control timescale," *IEEE Access*, to be published. DOI: 10.1109/ACCESS.2023.3316015.
[30] C. Yin, F. Li, "Reactive power control strategy for inhibiting transient overvoltage caused by commutation failure," *IEEE Trans. Power Syst*., vol. 36, no. 5, pp. 4764-4777, Sept. 2021.

SHUCHAN HE received the B.Eng. degree from the School of Electrical and Engineering, Huazhong University of Science and Technology (HUST), Wuhan, China, in July 2016. He is currently working toward the Ph.D. degree with the State Key Laboratory of Advanced Electromagnetic and Technology, School of Electrical and Electronic Engineering, Huazhong University of Science and Technology, Wuhan, China.

His current research interests include control and dynamic analysis of power systems with renewable power generations and high voltage dc (HVDC) transmission, in particular on modeling and dynamic analysis of HVDC converter station.

XIAOMING YUAN (S'97-M'99-SM'01) received the B.Eng. degree from Shandong University, Jinan, China, in 1986, the M.Eng. degree from Zhejiang University, Hangzhou, China, in 1993, and the Ph.D. degree from the Federal University of Santa Catarina, Florianópolis, Brazil, in 1998, all in electrical engineering.

From 1986 to 1990, he was with Qilu Petrochemical Corporation, China, where he was involved in the commissioning and testing of relaying and automation devices in power systems, adjustable speed drives, and high-power UPS systems. From 1998 to 2001, he was a Project Engineer with the Swiss Federal Institute of Technology Zurich, Switzerland, where he worked on flexible-ac-transmission systems and power quality. From 2001 to 2008, he was with GE GRC Shanghai as the Manager of the Low Power Electronics Laboratory, Shanghai, China. From 2008 to 2010, he was with GE GRC US as an Electrical Chief Engineer in Fairfield, USA. Since 2010, he has been a Professor of the State Key Laboratory of Advanced Electromagnetic Engineering and Technology, and the School of Electrical and Electronic Engineering, Huazhong University of Science and Technology, Wuhan, China. His research field includes stability and control of power system with multi-converters, control and grid integration of renewable energy generations, and control of high-voltage dc transmission systems.

Dr. Yuan is Distinguished Expert of National Thousand Talents Program of China, and Chief Scientist of National Basic Research Program of China (973 Program). He received the first prize paper award from the Industrial Power Converter Committee of the IEEE Industry Applications Society in 1999.

JIABING HU (S'05-M'10-SM'12) received the B. Eng. and Ph.D. degrees from the College of Electrical Engineering, Zhejiang University, Hangzhou, China, in 2004 and 2009, respectively. From 2007 to 2008, he was funded by Chinese Scholarship Council as a Visiting Scholar with the Department of Electronic and Electrical Engineering, University of Strathclyde, Glasgow, U.K. From April 2010 to August 2011, he was a Postdoctoral Research Associate with Sheffield Siemens Wind Power (S2WP) research center and the Department of Electronic and Electrical Engineering, University of Sheffield, Sheffield, U.K. Since September 2011, he has been a Professor with the State Key Laboratory of Advanced Electromagnetic Engineering and Technology, and School of Electrical and Electronic Engineering, Huazhong University of Science and Technology, Wuhan, China. His current research interests include grid-integration of large-scale renewables, and modeling, analysis and control of power electronized power systems.

Dr. Hu serves as an Editor of IEEE Transactions on Energy Conversion, an Associate Editor of IET Renewable Power Generation, and a member of Editorial Board for Automation of Electric Power Systems. He is the co-convenor of IEC SC8A JWG5 and an active expert of IEC SC8A WG1/AHG3. He was nominated in 2016, 2017 and 2018 by Elsevier to be between the 40 Most Cited Chinese Researchers in electrical and electronic engineering. He is the Fellow of Institute of Engineering and Technology (IET).

HUI YANG received the B.Eng. and Ph.D. degrees from the School of Electrical and Electronic Engineering, Huazhong University of Science and Technology (HUST), Wuhan, China, in 2014 and 2021, respectively. From 2021 to 2023, she has been a Postdoctoral Research Associate with HUST. Her current research interests include representations of AC voltage, current, and active/reactive power, in particular on active/reactive power analysis in the AC three-phase power system dynamics.